



**Geo-hydraulic characterization of a coastal aquifer system in South-eastern Nigeria with the inverse slope method**

**Ndifreke I. Udosen<sup>\*</sup>, Aniekan M. Ekanem, Jewel E. Thomas**

Received: November 6, 2023 / Accepted: January 3, 2024

© REJOST 2024

**Abstract**

Geophysical surveys were undertaken to determine the geo-hydraulic properties within a major coastal aquifer in Eket, South-eastern Nigeria. Information about geo-hydraulic properties of an aquifer are critical in the management and conservation of groundwater resources, hence it was necessary to characterize this major aquifer's geo-hydraulic properties. Geo-electrical data was acquired with the Schlumberger configuration and interpreted using the inverse slope method. The interpretation of the geo-electrical data as undertaken by the inverse slope method correlated with lithological information from well logs obtained close to the study area and indicated the presence of three geological layers (motley topsoil, fine sand, and coarse sand).

---

✉ Ndifreke Udosen: [ndifreke.udosen@yahoo.com](mailto:ndifreke.udosen@yahoo.com)

Department of Physics, Akwa Ibom State University,  
Mkpat Enin, Nigeria

---

Resistivity values of the overburden were noticeably higher than those of underlying layers, and the resistivity of the subsurface layers ranged from 0.5- 434  $\Omega$ m. A performance evaluation of the aquifer was carried out via quantitative characterization of the geo-hydraulic properties which included bulk resistivity, water resistivity, porosity, formation factor, hydraulic conductivity, transmissivity, permeability and tortuosity. Contour plots were generated to show how these geo-hydraulic parameters varied across the study area and empirical formulations were developed to aid in the modeling of aquifer properties in locations with similar geology. This work shows that the inverse slope method is an efficient method for interpreting resistivity data acquired from heterogeneous environments.

**Keywords:** Aquifer; Electrical Resistivity Surveying; Hydraulic parameters; Groundwater; Eket

## 1.0 Introduction

The knowledge of an aquifer's hydraulic properties is very critical in the management of groundwater resources (Soupious *et al.*, 2007; George *et al.*, 2017). These important hydraulic properties include porosity, formation factor, hydraulic conductivity, transmissivity, permeability, and tortuosity. Within the earth's subsurface are rocks with varying values of porosity and permeability. In order for a rock to be considered a productive aquifer, its matrix must have excellent porosity and permeability.

A rock's porosity is a measure of the void spaces within the rock. Excellent porosity is important because groundwater flows within the rock's pore spaces. The permeability of a rock matrix is influenced by the geometry of the pores, the size and shape of the grains and soil sediments, the cementation exponent, the type of subsurface rock, how saturated the subsurface layer is with water, and the environment in which these sediments are deposited (Ibuot and Obiora, 2021; Abed, 2014; Abuseda *et al.*, 2015). Information about a rock's permeability may be acquired via permeability tests on core plugs (George *et al.*, 2017). The hydraulic conductivity and transmissivity of the aquifer will then be derived from the results obtained from the pumping tests. Hydraulic conductivity and transmissivity are interconnected as they influence the rate of groundwater flow within the aquifer. These two parameters serve as indicators of the ability of an aquifer to allow the flow of water over both a unit thickness of the aquifer and its entire saturated thickness. Tortuosity is dependent on the hydraulic conductivity and permeability. A high tortuosity entails a low effective porosity (George *et al.*, 2011). Via analysis of the grain sizes and permeability measurements taken in the laboratory, one can obtain information about the aquifer's hydraulic conductivity and

transmissivity (Sattar *et al.*, 2016). The problem with determining these parameters from pumping tests and well information is that these procedures are typically very expensive, they require much labor, and are very time consuming. Furthermore, due to the heterogeneity within the earth's subsurface, the hydraulic properties of an aquifer obtained from a certain borehole within a certain location could give information very different from that obtained from another borehole a little farther off (Inim *et al.*, 2020; Udosen and George, 2018b; Udosen, 2022).

Consequently, electrical resistivity methods have been used and found to be effective in characterization of aquifer hydraulic parameters (Niwas *et al.*, 2011; Uwa *et al.*, 2019; Ekanem *et al.*, 2020). The geo-electric method enables one to determine the bulk resistivity, the thickness, and the depth of subsurface layers. Using empirical formulas, these geo-electric parameters are used in the determination of the aquifer's hydraulic properties. Apart from its effectiveness, electrical resistivity surveying is a non-invasive methodology that does not damage the subsurface in any way (Udosen and George, 2018a; Udosen and Potthast, 2018c).

In this work, electrical resistivity surveying was applied to determine important hydraulic properties of a coastal aquifer with the inverse slope method (Narayan and Ramanujachary, 1967; George *et al.*, 2022) in Eket, South-Eastern Nigeria. In the past, the residents within the study area had as a major means of potable water, the surface water such as streams and lakes. In the present era however, there has been an exponential increment in the population and a consequent increase in industrial activities within the area, leading to an increment in the water requirements within the study area.

Consequently, the region is experiencing degradation in the quality of surface water available for industrial and domestic purposes. This study aimed at evaluating the hydraulic properties of the aquifer within this area with electrical resistivity surveying. Although aquifer characterization is linked to groundwater potentiality, there has been no recent study within the study area aimed at characterizing the geo-hydraulic parameters of this aquifer system. Such important information will aid in the development of effective governmental policies on groundwater management and conservation within the study area. The inverse slope method was used as the interpretative technique in order to assess the method's suitability in highly heterogeneous environments, such as the study area, and compare its results with those obtained from borehole lithological logs. Compared to conventional inversion methods, the inverse slope method has the capability of delineating thin layers and avoiding the limitations of the principles of suppression and equivalence within geo-layers (Asfahani *et al.*, 2023; George *et al.*, 2022).

## 2.0 Location and Geology of Study Area

This work was carried out in Eket Local Government Area, which lies between Latitudes 4.33" and 4.45" and Longitudes 7.52" and 8.02". The study area lies within the east of the Niger delta region in Southern Nigeria (Figures 1 and 2). Eket has an area of approximately 214 km<sup>2</sup> and can be accessed through crisscrossing roads which span the area. It is bordered by Nsit Ubium Local Government on the north, Ibeno Local Government on the south, Esit Eket Local Government on the east, and Onna Local Government area on the west. Eket has a tropical humid climate with two major climatic seasons:

the dry season (November–March) and the wet season (April–October). The annual rainfall in the area is approximately 3040mm and the average annual temperature ranges between 23° to 31° C. Eket is drained by Kwa Iboe River alongside the tributaries of this river.

With regards to geology, the main sediments underlying Eket are the recent Tertiary sands, which are of the Benin Formation (or Coastal Plain Sands). The Benin Formation is the topmost layer in the Niger Delta Region, and is made of sand and gravels. It is also the water-bearing unit in the study area. The sands of the Benin formation are poorly sorted and have varying grain sizes, some grains being fine, and others being coarse (Short and Stauble, 1967). There are locations where inter-beddings of lignite, clay, silt and sandstone occur within the Benin Formation (Reijers and Petters, 1987). As a result of these inter-beddings, there exist locations having multiple aquifer units (Okereke *et al.*, 1998; Esu *et al.*, 1999; Edet and Okereke, 2002). Underlying the Benin Formation is the Agbada Formation, the hydro-carbon bearing unit within the Niger Delta region (Short and Stauble, 1967; Avbovbo, 1978; Stacher, 1995).

## 3.0 Material and Methods

Geo-electrical methods were employed to delineate the lithology and vertical/lateral electrical properties within the highly heterogeneous subsurface within the study area. Resistivity surveying methods are based on the premise that when current is injected into the subsurface, it penetrates the ground and the current's penetrative depth increases with the spacing between the current electrodes. Hence, inhomogeneities lying deep within the subsurface will influence the electrical potential distribution within the VES soundings.



Electrical current was injected through electrodes A and B placed at varying locations over the study area. Another pair of potential electrodes M and N was used to determine the variations of the potential field, when current was being injected through A and B. The non-homogenous overburden overlying the aquifer may cause discrepancies observed within the sounding data. In locations where the sounding data was anomalous, the soundings were repeated and the electrode orientation changed. To avoid errors within the data, it was ensured that the electrode-ground contact was excellent. One is more prone to have problems with poor-electrode ground contact in locations comprising gravels, waste materials, and pebbles. Wherever such anomalous materials were found, they were removed to enable good electrode-ground contact. From the geo-electrical data, lithological information was obtained and this was correlated with information from well logs (Ibuot *et al.*, 2017) obtained close to the study area.

To acquire data for this study, ten vertical electrical soundings were undertaken in the study area with the use of the Schlumberger array having a maximum profile length of 400m. The Schlumberger array was used on the field due to its excellent resolution of vertical structures and its ability to penetrate deeper into the subsurface compared to other electrode configurations. The minimum half potential electrode spacing ( $MN/2$ ) was 0.25m while the maximum spacing was 20m. On the other hand, the minimum half current electrode spacing ( $AB/2$ ) was 1m while the maximum spacing was 400m. The field equipment used was the ABEM SAS 1000 resistivity meter. The resistivity meter alongside its accessories served to inject a known current into the subsurface via the two current electrodes A and B. The resulting electric potential gradient

was detected using the two potential electrodes M and N. The resistivity meter uses Ohm's law:

$$R_a = \frac{V}{I} \quad (1)$$

to generate values of apparent resistance  $R_a$  of the earth's subsurface layers. The apparent resistance data was transformed into apparent resistivity information with the formula

$$\rho_a = \Pi \left[ \frac{\left(\frac{AB}{2}\right)^2 - \left(\frac{MN}{2}\right)^2}{MN} \right] \cdot R_a \quad (2)$$

The inverse slope method (Kouassi *et al.*, 2017; Bouadou *et al.*, 2019; Al-Fares and Asfahani, 2018; Shekhawat and Chundawat, 2011; Mohamed *et al.*, 2014) was then used to invert the sounding data acquired with the Schlumberger array. After acquisition of the field data, the values of  $\frac{AB}{2} / \rho_a$  were plotted against the values of  $AB/2$ . The resulting graph would have line segments that would indicate the number of layers within the subsurface. To determine the true resistivity  $\rho$  of a given layer, the equation used was

$$\rho = \frac{1}{|S_i|} \quad (3)$$

where  $S_i$  represented the slope of that segment. To determine the depth of each layer, the equation used was

$$d_n = \frac{(I_{n+1} - I_n)}{(S_n - S_{n+1})} \times \frac{2}{3} \quad (4)$$

where  $S$  = the slope of the line segment,  $I$  = intercept of the line segment, and  $n$  = layer number. The advantage of the inverse slope method over conventional methods is that even in cases where there are thin layers buried at great

depths, the method is still capable of delineating those thin layers so far as the injected current can extract signals from the target layers. In previous studies (Aretouyap *et al.*, 2019, Aretouyap *et al.*, 2021), when the curve matching method was applied in the evaluation of aquifer hydraulic parameters, the resolution of thin layers obtained with curve matching was so poor that such layers were simply not delineated. Hence, the inverse slope method was applied in this work to overcome the problem of indistinguishable thin layers obtained by curve matching methods. Further, the inverse slope method helps overcome the problem of suppression and equivalence, especially when the data interpretation is constrained by well logs (Asfahani *et al.*, 2023). In addition, when the geo-layers are heterogeneous, the curve matching method has been found to give inaccurate results. In previous studies (George *et al.*, 2022; Asfahani *et al.*, 2023), the inverse slope method was shown to have greater sensitivity than curve matching methods and also generated results that correlated better with lithological well logs than the conventional computer-based least-square inversion schemes.

The inverse slope method was first developed by Narayan and Ramanujachary (1967) and it was then used to invert resistivity sounding data obtained from the Wenner array configuration. Under this approach, the inverse of resistance (i.e., conductance) was plotted against the equal electrode spacing "a" employed in the Wenner array. The number of subsurface layers was taken to be the number of linear segments on the plots. The depth of the subsurface layers was defined by the points of intersection between one line segment and a successive line segment. The true resistivity of the subsurface layer was defined by the slope of each line segment.

The inverse slope method is easier to use than curve-matching (Asfahani *et al.*, 2023) and has been extended to other electrode configurations (Mohamed *et al.*, 2014). It has been found to be an effective method for use in the interpretation of resistivity data (Rao *et al.*, 2005; Babar and Muley, 2018; Yadav *et al.*, 2009; Asfahani, 2016; Asfahani, 2013). It is especially useful in the delineation of thin layers and has been found capable of identifying such layers regardless of how thin the layer may be (Asfahani *et al.*, 2023).

#### 4.0 Results and Discussion

The inverse slope method is easy to use, cost-effective, and able to delineate between different lithological zones via measures of subsurface resistivity and depth obtained directly from regression curves. Due to subsurface heterogeneity and consequently wide variations in resistivity distribution within the surveyed area, it was important to use well logs to generate information about the lithology of the surface area. The goal of the resistivity surveying method was to delineate the geological conditions of the survey area and determine the location of saturated formations and their respective depths. A mapping of the lithological layers is easier when the subsurface has horizontal layering and is approximately isotropic. In locations where the lithology is heterogeneous and boundaries between lithological layers are not parallel or well-defined, there tends to be an overlap of one layer into the other, and field data needs to be constrained with borehole information. To generate information about the potentiality of the aquifer that would aid in its conservation and management, it was therefore important for geophysical, aquifer performance, and lithological information to be incorporated to acquire information about the aquifer characteristics.

The regression plots obtained from the inverse slope method were used to estimate the geo-electric parameters. An example of such a plot is illustrated in Figure 3. The linear segments for all 10 VES profiles had coefficients of determination  $R^2$  ranging from 0.81 – 1.00 for all the profile lines, implying a good model fit. The inverse

slope method enabled one to distinguish between motley topsoil, fine sand and coarse sand (Figure 4) and this correlated with lithological information obtained from borehole drilling data obtained during previous work carried out in the study area (Ibuot *et al.*, 2017).

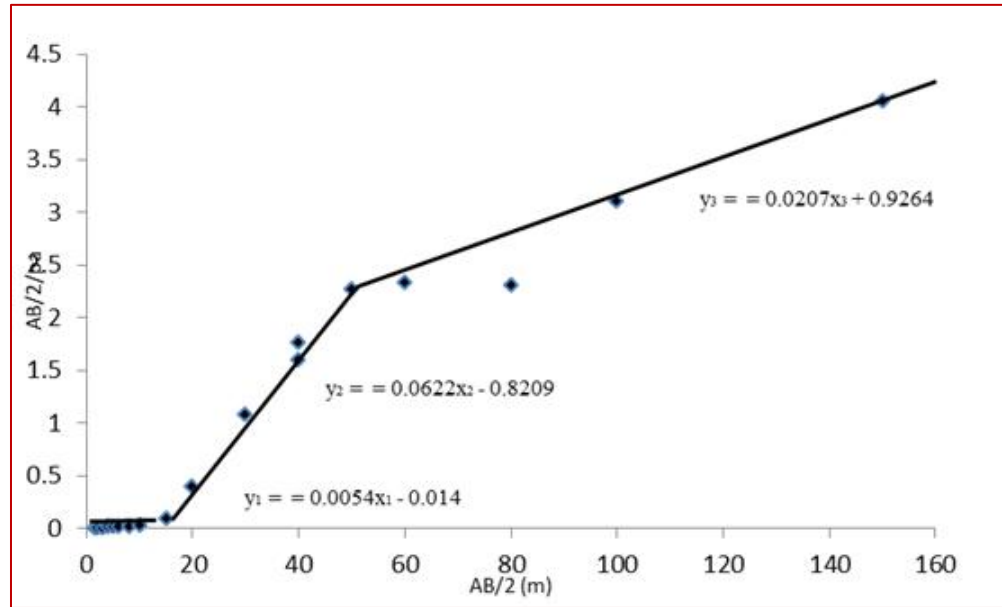


**Figure 3:** Regression plot for the inverse slope method used in the determination of geo-electric parameters for VES 3.

The VES interpretations (Table 1) indicates that the study area comprises 3 geo-electrical layers which correspond to motley topsoil, fine sand and coarse sand. The first layer has a resistivity distribution ranging from 22 - 434  $\Omega\text{m}$  and a thickness varying from 1.45 – 22.00 m. The lateral variations in resistivity within the layer are due to subsurface heterogeneity. The second layer has resistivity values ranging from 1.8 -131  $\Omega\text{m}$  and a thickness varying from 9.4 – 46.7 m. The third layer's resistivity distribution ranged from 0.5 to 41.7  $\Omega\text{m}$ . It is possible that locations with wide lateral variations indicate diversity in geo-materials underlying the overburden. Data generated from the VES soundings were

correlated with borehole lithological well information. According to well data, the water table is found at a depth of 16 m. The study area does present problems of saline groundwater as it is not shadowed directly by the coastline. From data on the resistivity of different kinds of geologic materials (Gopalan, 2011), fracture rocks comprising saline water have resistivity values of 0.1 - 0.2 $\Omega\text{ m}$ ; clay, silt and sand have resistivity values < 15  $\Omega\text{m}$ ; fine and medium grained sands have resistivity values of 15 – 30  $\Omega\text{m}$ ; medium and coarse sands have resistivity values of 30 - 60  $\Omega\text{m}$ ; highly fractured rocks with water have resistivity values of 60-100  $\Omega\text{m}$ ; fractured rocks comprising water have resistivity

values of 100-200  $\Omega\text{m}$ , minimally fractured rocks have resistivity values of 200 - 300  $\Omega\text{m}$ ; massive rock has resistivity values  $> 300 \Omega\text{m}$ , and laterites have resistivity values  $> 2000 \Omega\text{m}$ .

The materials within the study area, from their resistivity values, are found to comprise fine/medium grained sands and coarse sand.

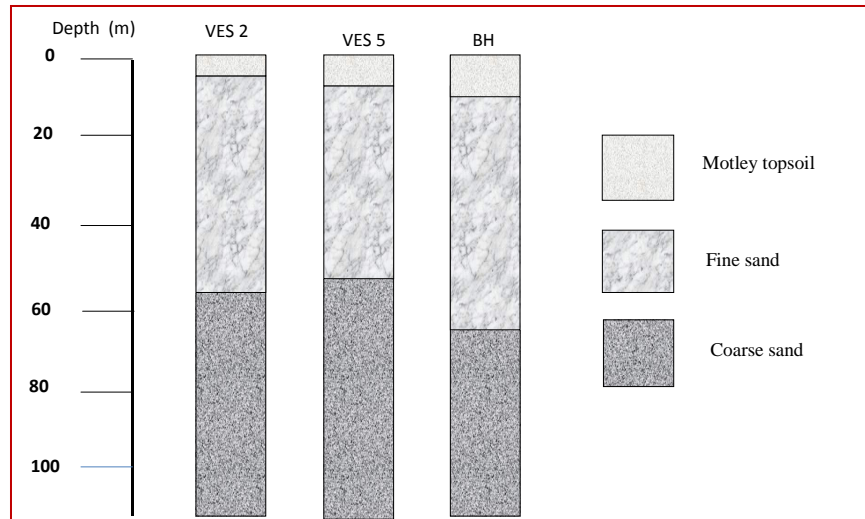


**Figure 4:** Borehole lithology correlating to VES data points

**Table 1:** Resistivity, thickness and depth information for each geo-electric layer obtained from the inverse slope method

VES NO	Latitude (°)	Longitude (°)	Bulk Resistivity ( $\Omega\text{m}$ )			Thickness (m)		Depth (m)		Elevation (m)
			$\rho_1$	$\rho_2$	$\rho_3$	$h_1$	$h_2$	$d_1$	$d_2$	
1	4.61550000	7.93575000	200.00	30.01	23.04	10.06	41.15	10.06	51.21	11
2	4.61644444	7.93358333	250.00	29.76	0.53	1.45	55.78	1.45	57.23	16
3	4.61633333	7.93350000	434.78	15.77	2.59	9.43	18.28	9.43	27.71	17
4	4.61619444	7.93338889	370.37	1.80	1.70	4.74	35.49	4.74	40.23	16
5	4.61613889	7.93327778	192.31	55.25	0.66	5.7	46.69	5.70	52.39	15
6	4.61488889	7.93561111	42.55	33.33	1.97	22.02	12.62	22.02	34.64	14
7	4.61483333	7.93558333	22.94	45.54	83.33	0.07	9.40	0.07	9.47	20
8	4.61486111	7.93552778	32.15	80.65	0.66	9.49	24.03	9.49	33.52	16
9	4.61494444	7.93558333	48.54	131.58	0.66	2.47	23.28	2.47	25.75	21
10	4.61527778	7.93597222	256.41	70.92	41.66	14.43	45.97	14.43	60.40	19

The map of the distribution of aquifer bulk resistivity  $\rho_b$  within the study area is shown in Figure 5. Low resistivity values of about 10-50  $\Omega\text{m}$  are observed in the northern parts of the study site. To determine the hydraulic properties

of the aquifer, one needs to compute water resistivity. An empirical formulation  $\rho_w = 0.0577\rho_b + 13.643$  (Ibanga and George, 2016) determined from an area with similar



geology was applied to compute water resistivity (see Figure 6). A comparison of Figures 5 and 6 shows that locations with high values of aquifer bulk resistivity are locations of high water resistivity. Aquifer hydraulic properties were then computed (Table 2). The hydraulic properties of an aquifer provide insights into

aquifer behavior and enable the development of quantitative and qualitative models which are important in groundwater management and conservation. The properties investigated in this work were the porosity, the formation factor, the hydraulic conductivity, the transmissivity, the permeability, and the tortuosity.

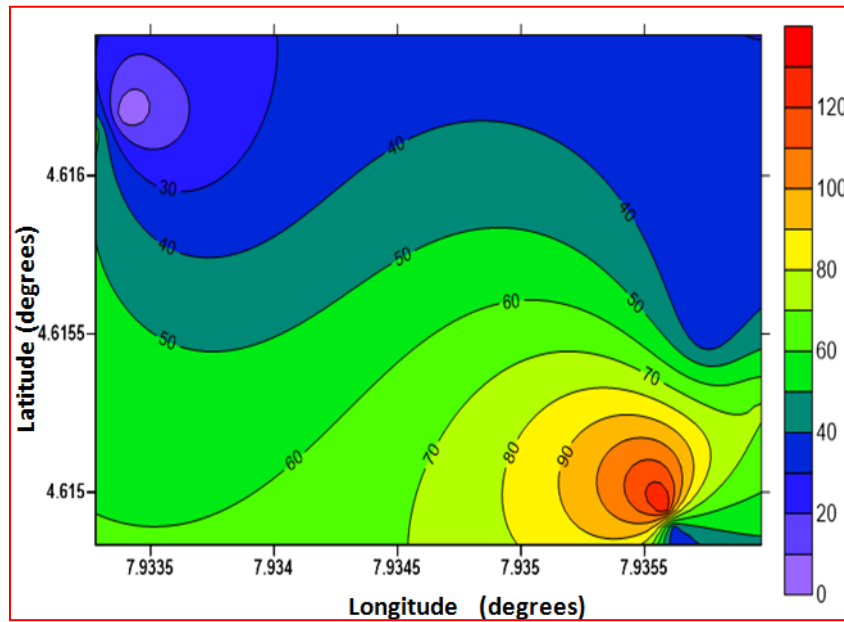


**Figure 5:** Map showing the distribution of aquifer bulk resistivity within the study area

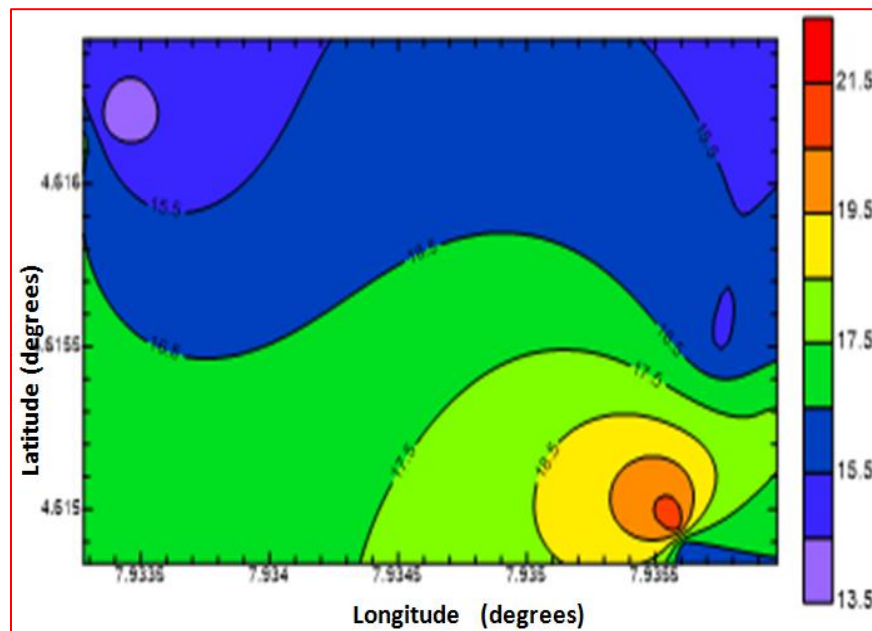


**Figure 6:** Map showing the distribution of water resistivity within the study area

Table 2: Aquifer hydraulic parameters derived from geo-electrical information

VES NO	Bulk resistivity $\rho$ ( $\Omega\text{m}$ )	Thickness $h_a$ (m)	Water resistivity $\rho_w$ ( $\Omega\text{m}$ )	Formation factor F	Porosity $\Phi$	Hydraulic conductivity K (m/day)	Transmissivity T ( $\text{m}^2/\text{day}$ )	Permeability $K_p$ (mD)	Tortuosity $\tau$
1	30.01	41.15	15.38	1.95	0.43	96.22	3959.63	161213.00	0.91
2	29.76	55.78	15.36	1.94	0.43	98.33	5484.76	164738.00	0.91
3	15.77	18.28	14.55	1.08	0.62	705.47	12896.00	1181932.00	0.82
4	1.80	35.49	13.75	0.13	2.46	2842.66	100886.00	4762559.00	0.57
5	55.25	46.69	16.83	3.28	0.30	23.81	1111.75	39893.30	1.00
6	33.33	12.62	15.57	2.14	0.40	73.84	931.90	123716.00	0.93
7	45.54	9.4	16.27	2.80	0.34	35.79	336.47	59969.20	0.97
8	80.65	24.03	18.30	4.41	0.25	11.59	278.57	19422.40	1.05
9	131.58	23.28	21.24	6.19	0.20	5.26	122.38	8807.42	1.12
10	70.92	45.97	17.74	4.00	0.27	14.64	673.17	24534.00	1.04

Porosity ( $\Phi$ ) is typically expressed as the ratio of pore volume to the bulk rock volume. The ability of the aquifer to store water is a function of porosity. Porosity is dependent on several parameters such as the sorting of the grains, the cementation exponent, the grain geometry and the grain size. The porosity of a rock matrix can be determined from the formation factor F with the use of Archie's equation (Archie, 1942) which is given as

$$F = \frac{\rho_b}{\rho_w} = a\phi^{-m} \quad (5)$$

where  $\rho_b$  = aquifer bulk resistivity  $\rho_w$  = water resistivity,  $a$  = geometrical factor of the pores, and  $m$  = cementation factor. To compute porosity, Archie's equation was applied and values used for Archie's parameters were pore geometry  $a = 0.5245\text{m}$ , cementation factor  $m = 1.5432$ , and mean grain size  $d_m = 0.000348\text{m}$  (George et al., 2011). The value for dynamical viscosity for fine and coarse sands,  $\mu_d = 0.0014\text{kg/ms}$  (Fetter, 2018) was used since the lithology of the study area comprises coarse and fine sands. The density of water was taken as

$1000\text{kg/m}^3$ . The distribution map for the formation factor (Figure 7) showed that the formation factor varied from 1.0 to 5.0 with particularly low values in the northern section of the study area. The distribution map for porosity (Figure 8) showed that porosity is the inverse of formation factor F. Locations where the formation factor F was low were locations where the porosity  $\Phi$  was high. The southern parts of the study area had particularly low values of porosity ( $< 40\%$ ). The hydraulic conductivity K, otherwise known as the co-efficient of permeability, is an important factor that influences groundwater transmission through an aquifer system. The hydraulic conductivity defines the aquifer's ability to allow the flow of water under a hydraulic gradient (Lobo-Ferreira et al., 2005). To determine the hydraulic conductivity, the Kozeny-Carmen-Bear equation (Domenico and Schwartz, 1997) was used and it is given as:

$$K \approx \left( \frac{\delta_w g}{\mu_d} \right) \left( \frac{d_m^2}{180} \right) \left( \frac{\phi^3}{(1-\phi)^2} \right) \quad (6)$$

where  $\delta_w$  = density of water,  $\mu_d$  = dynamic viscosity of water,  $d_m$  = mean grain size,  $\phi$  = porosity and  $g$  = acceleration due to gravity.

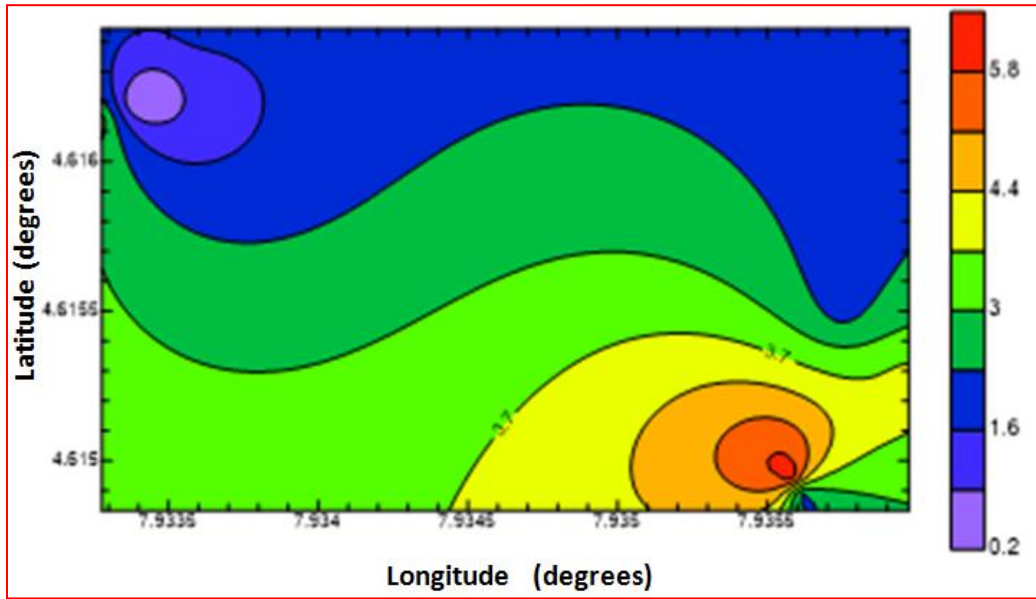


**Figure 7:** Map showing the distribution of formation factor within the study area

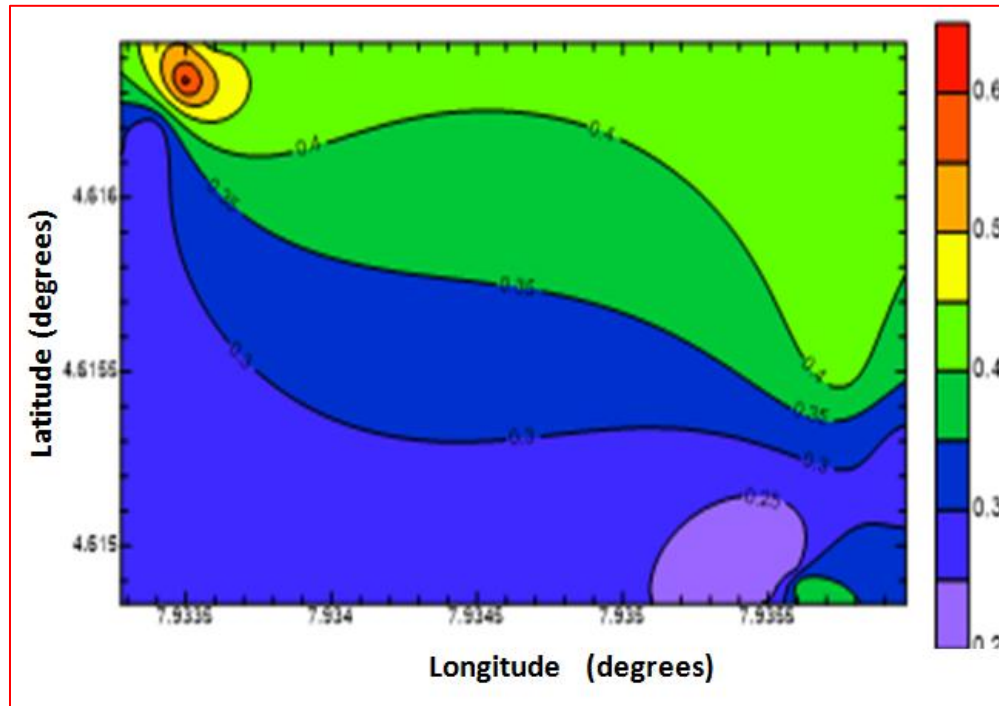


**Figure 8:** Map showing the distribution of porosity within the study area

The rate at which groundwater flows, depends on conductivity. The greater the value of the the hydraulic gradient and the hydraulic hydraulic conductivity, the faster groundwater

flows through the porous media. Figure 9 shows the distribution map for hydraulic conductivity  $K$  and indicates high values of  $K$  in the north-western parts of the study area.

Transmissivity  $T$  is an important parameter that estimates the capacity of the aquifer to allow groundwater transmission. The transmissivity is defined as the rate at which groundwater flows through a unit of cross section under a hydraulic gradient over the entire saturated aquifer thickness (Bear, 2012). The transmissivity of an aquifer is dependent on the geometry, the quantity of pore throats, and the interconnectivity of the pore throats within the rock matrix. The relationship between transmissivity  $T$  and hydraulic conductivity  $K$  is given by:

$$T = Kh \quad (7)$$

where  $h$  denotes the thickness of the aquifer layer. Whereas transmissivity investigates groundwater flow throughout the entire thickness of the aquifer, hydraulic conductivity investigates groundwater flow for a unit thickness of the aquifer. High values of transmissivity denote greater ability to transmit groundwater and low values denote lesser ability to transmit groundwater. Figure 10 shows the transmissivity distribution map. A comparison of the hydraulic conductivity distribution map with the transmissivity distribution map shows a linear relationship between hydraulic conductivity and transmissivity. Locations of high conductivity are also locations of high transmissivity and locations of low hydraulic conductivity are also locations of low transmissivity.

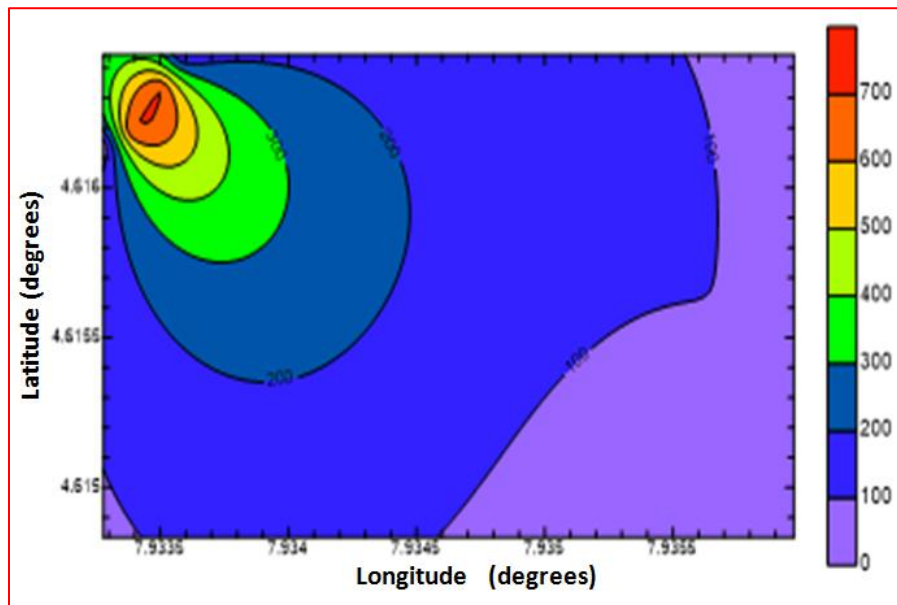


**Figure 9:** Map showing the distribution of aquifer hydraulic conductivity within the study area

Permeability is one of the rock's properties that defines its ability to allow fluid flow. Permeability has a relationship with porosity; however, it does not depend on the porosity of the rock formation. Permeability is dependent on the size and

interconnectivity of the pore spaces within the rock. Permeability  $K_p$  and hydraulic conductivity  $K$  are related by:

$$K_p = \frac{K\mu_d}{\delta_w g} \quad (8)$$

where  $\delta_w$  = density of water,  $\mu_d$  = dynamic viscosity of water, and  $g$  = acceleration due to gravity.

Equation (8) implies that permeability varies directly as the hydraulic conductivity. The permeability and effective porosity of a rock matrix determines how much groundwater is abstracted from the subsurface in hydrogeological aquiferous units. Whenever there is high permeability, groundwater moves quickly within the aquifer. Figure 11 shows the distribution map for permeability with high values of permeability in the northern parts of the study area.

Tortuosity  $\tau$  is an important hydraulic parameter of an aquifer and it is given as the ratio of the length of the path of groundwater flow to the linear distance between the ends of the path of groundwater flow (Bear, 2012). Tortuosity is related to the porosity and formation factor via:

$$\tau = \sqrt{F\phi} \quad (9)$$

The distribution map for tortuosity (Figure 12) shows values ranging from 0.9 - 1.1. A comparison of the permeability distribution map with the tortuosity distribution map shows an inverse relationship. Locations of high permeability are locations with low values of tortuosity.

The regression curve showing the relationship between permeability  $K_p$  and porosity  $\Phi$  is shown in Figure 13. The relationship between the two parameters is given by

$$\Phi = 0.0203K_p^{0.2546} \quad (10)$$

with a coefficient of determination  $R^2 = 0.998$ , which implies that the statistical model predicts the outcome. The regression curve showing the relationship between tortuosity  $\tau$  and permeability  $K_p$  is shown in Figure 14.

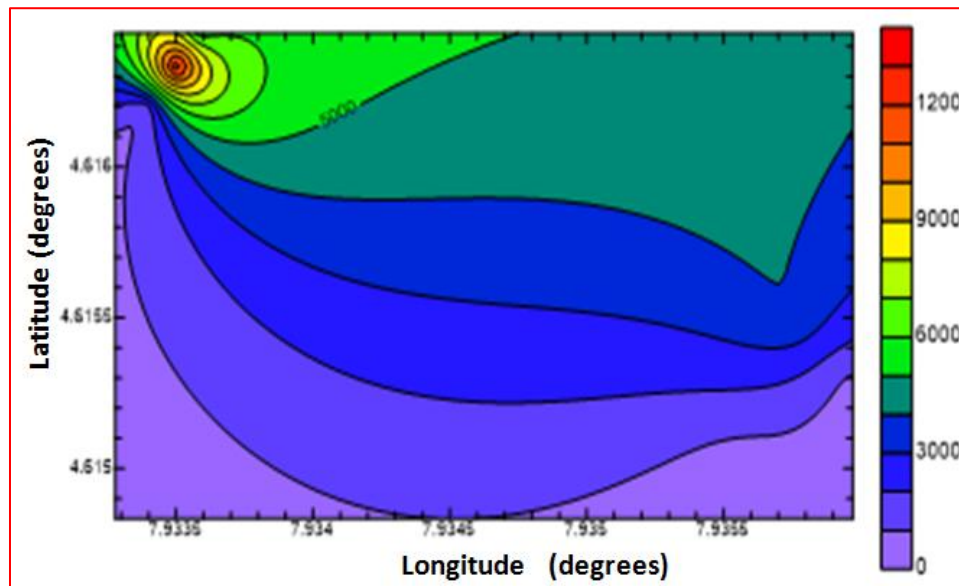


**Figure 10:** Map showing the distribution of aquifer transmissivity within the study area

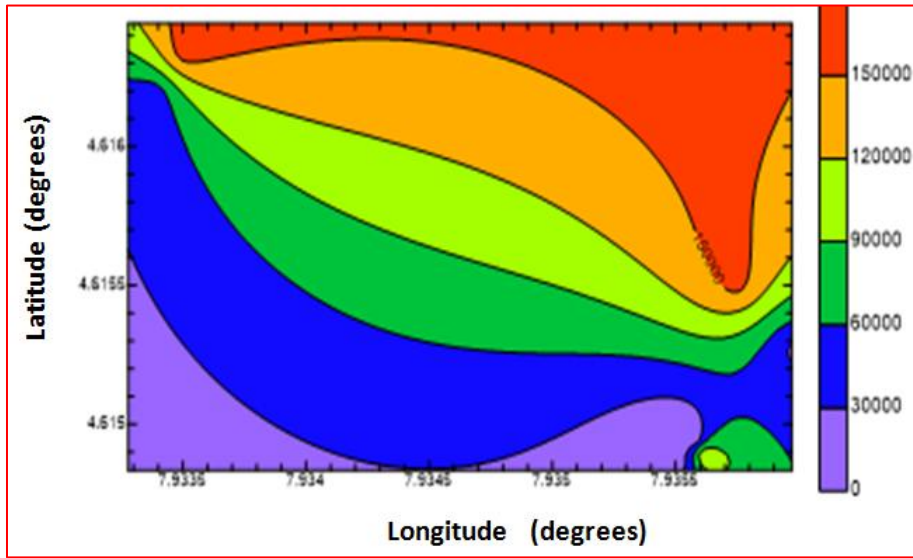


**Figure 11:** Map showing the distribution of aquifer permeability within the study area

The curve indicates an inverse relationship is observed between the two parameters, implying that a decrease in tortuosity corresponds to an increase in permeability and an increase in tortuosity corresponds to a decrease in permeability. The empirical relationship between the two parameters is given as:

$$K_p = 41678\tau^{-14.45} \quad (11)$$

and the coefficient of determination  $R^2 = 0.998$ . And finally, the regression curve of hydraulic

conductivity and porosity is indicated in Figure 15. The empirical relationship between the two parameters is given as

$$K = 4020\Phi^{4.2629} \quad (12)$$

and the coefficient of determination  $R^2 = 0.991$ . From the plot, it can be seen that a linear relationship exists between the two parameters implying that the greater the porosity, the greater the hydraulic conductivity of the aquifer.

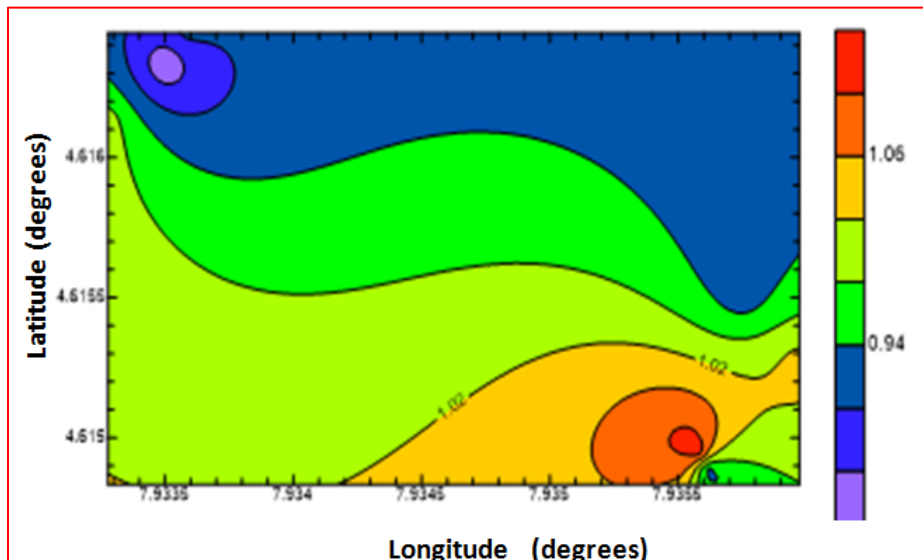


**Figure 12:** Map showing the distribution of aquifer tortuosity within the study area

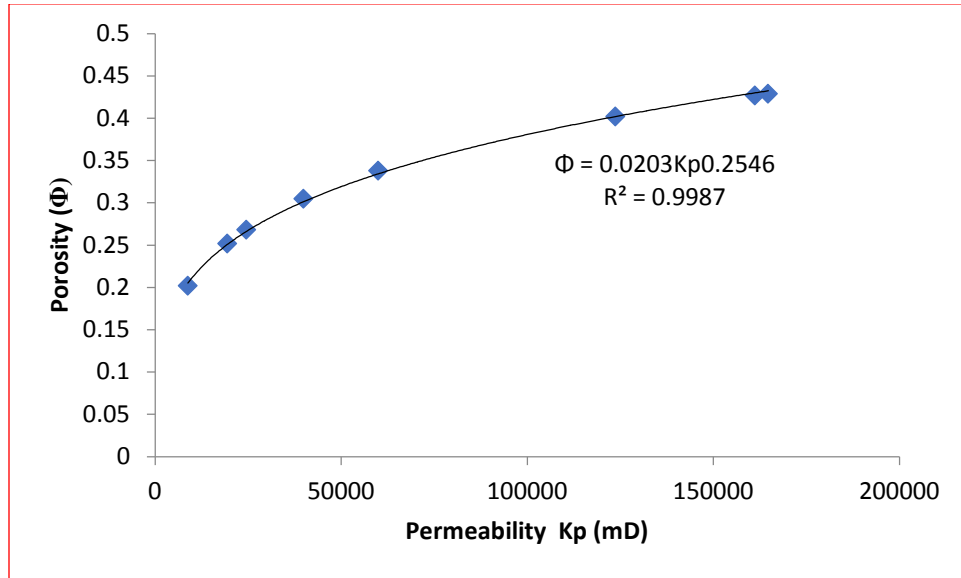


**Figure 13:** Regression curve showing relationship between permeability  $K_p$  and porosity  $\Phi$

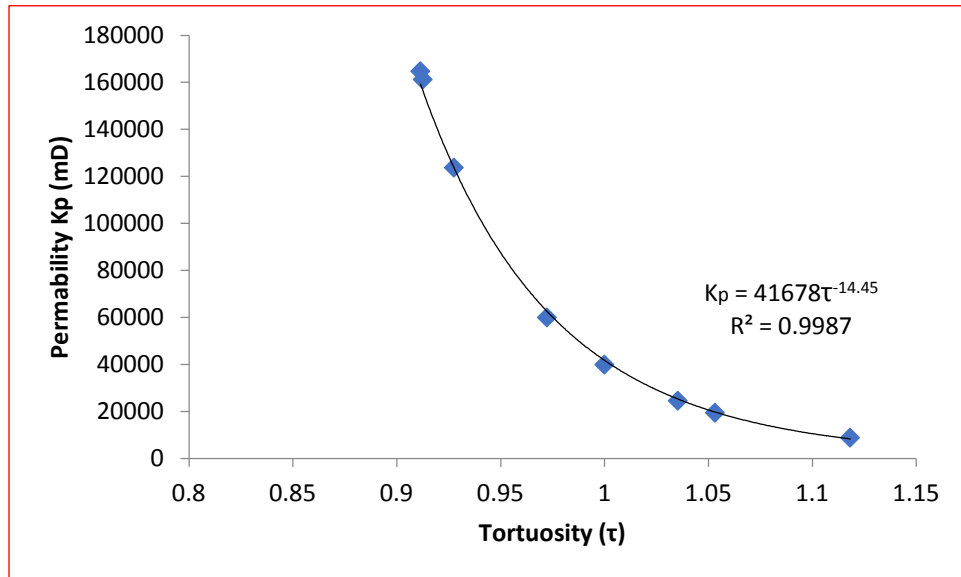


**Figure 14:** Regression curve showing relationship between tortuosity  $\tau$  and permeability  $K_p$

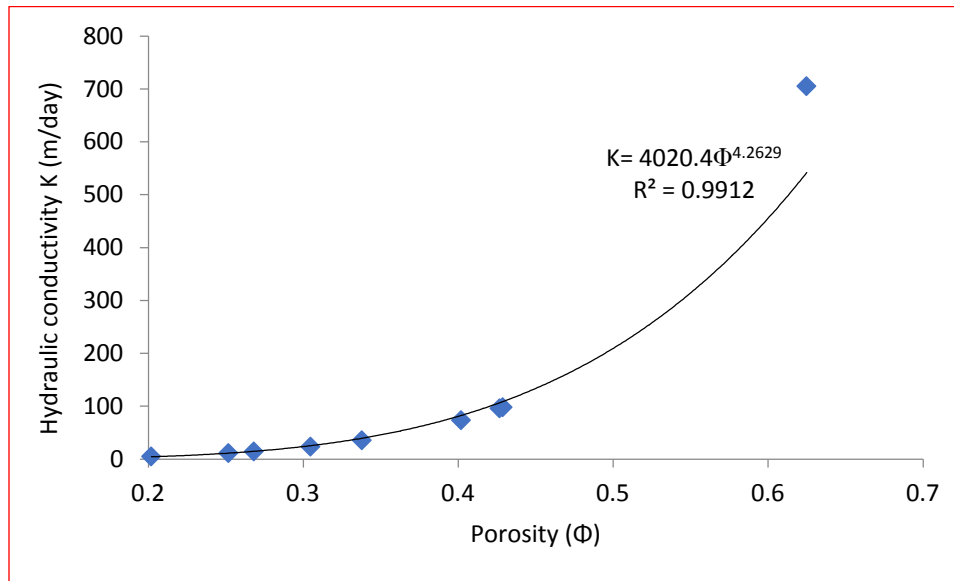


**Figure 15:** Regression curve showing relationship between porosity  $\Phi$  and hydraulic conductivity  $K$

### Conclusion

In this work, a non-invasive method, electrical resistivity surveying was applied to determine aquifer hydraulic parameters. With the use of ten profiles within the study area, VES was undertaken with the use of Schlumberger array configuration that applied a maximum electrode spacing of 400m. The field data acquired was interpreted with the inverse slope method to generate geo-electric parameters such as the true resistivity distribution, the thickness and the depth of each layer. With the use of empirical formulae, these geo-electric parameters were used to determine the hydraulic parameters of the aquifer. The lithology of the study area as determined from geo-electric data shows that the area is made up of sands that are poorly sorted and have varying grain sizes, some grains being fine, and others being coarse. Further, there are locations where inter-beddings of lignite, clay, silt and sandstone occur.

The regression plots of the various hydraulic parameters show a linear relationship between porosity and permeability, a linear relationship between porosity and hydraulic conductivity, and

an inverse relationship between permeability and tortuosity. From the regression plots, empirical formulas have been developed that will prove helpful in modeling aquifer properties in locations with similar geology. There exists immense heterogeneity and subsurface lateral variation within the study area, hence, resistivity information had to be correlated with nearby well logs to generate values of the approximate resistivity within the subsurface layers and also to give a more realistic image of the lithology. The thickness of the topmost layer and the underlying layers correlated with data obtained from the borehole. Comparison was made between geo-electrical sections obtained from the inverse slope method and well information and the data shows that the geo-electrical sections obtained from inverse slope correlates with well lithological information (Virupaksha and Lokesh, 2021). The operational ease of the inverse slope method lies in its ability to generate values of subsurface resistivity and depths directly from the regression curves of acquired field data. Another strong benefit of using the inverse slope method to distinguish different types of strata is that it can serve as a reference point for additional



geochemical research on the lithological variations within the study area. Using the inverse slope method in highly heterogeneous settings has proved the method's suitability in determination of various lithological sections. Hence, compared to logarithmic curve-matching, the inverse slope method is easier to apply and it offers numerous qualitative and quantitative benefits due to its display on a linear scale.

**Data availability statement:** Data will be made available on reasonable request

**Conflict of interest statement:** The authors declare that there is no conflict of interest.

## References

- Abed, A.A., 2014. Hydraulic flow units and permeability prediction in a carbonate reservoir, Southern Iraq from well log data using non-parametric correlation. *International Journal of Enhanced Research in Science Technology & Engineering*, 3(1), pp.480-486.
- Abuseda, H., Kassab, M.A., LaLa, A.M. and El Sayed, N.A., 2015. Integrated petrographical and petrophysical studies of some Eocene carbonate rocks, Southwest Sinai, Egypt. *Egyptian Journal of Petroleum*, 24(2), pp.213-230.
- Al-Fares, W. and Asfahani, J., 2018. Evaluation of the leakage origin in Abu Baara earthen dam using electrical resistivity tomography, northwestern Syria. *Geofísica internacional*, 57(4), pp.223-237.
- Archie, G.E., 1942. The electrical resistivity log as an aid in determining some reservoir characteristics. *Transactions of the AIME*, 146(01), pp.54-62.
- Arétouyap, Z., Bisso, D., Njandjock Nouck, P., Amougou Menkpa, L.E. and Asfahani, J., 2019. Hydrogeophysical characteristics of Pan-African aquifer specified through an alternative approach based on the interpretation of vertical electrical sounding data in the Adamawa Region, Central Africa. *Natural Resources Research*, 28, pp.63-77.
- Aretouyap, Z., Bisso, D., Assatse, W.T., Kana, J.D., Ghomsi, F.E.K., Nouayou, R., Nouck, P.N. and Asfahani, J., 2021. A detailed analysis of hydro-parameters of the Adamawa Plateau watershed derived from the application of geoelectrical technique. *Environmental Earth Sciences*, 80, pp.1-11.
- Asfahani, J., 2013. Groundwater potential estimation using vertical electrical sounding measurements in the semi-arid Khanasser Valley region, Syria. *Hydrological sciences journal*, 58(2), pp.468-482.
- Asfahani, J., 2016. Inverse slope method for interpreting vertical electrical soundings in sedimentary phosphatic environments in the Al-Sharquieh mine, Syria. *CIM Journal*, 7(2), pp.93-104.
- Asfahani, J., Aretouyap, Z. and George, N., 2023. Hydraulic characterization of the Adamawa-Cameroon aquifer using inverse slope method. *Water Practice and Technology*, 18(3), pp.547-562.
- Avbovbo, A.A., 1978. Tertiary lithostratigraphy of Niger delta. *AAPG Bulletin*, 62(2), pp.295-300.

- Babar, M. and Muley, R., 2018. Investigation of sub-surface geology through integrated approach of geological and geophysical studies in the part of South-Eastern Maharashtra, India. *American J Water Res*, 6(3), pp.123-136.
- Bear, J., 2012. *Hydraulics of groundwater*. Courier Corporation.
- Bouadou, R.A.M., Kouassi, K.A., Kouassi, F.W., Coulibaly, A. and Gnagne, T., 2019. Use of the inverse slope method for the characterization of geometry of basement aquifers: case of the department of boua (ivory coast). *Journal of Geoscience and Environment Protection*, 7(06), p.166.
- Domenico, P.A. and Schwartz, F.W., 1997. *Physical and chemical hydrogeology*. John wiley & sons.
- Edet, A.E. and Okereke, C.S., 2002. Delineation of shallow groundwater aquifers in the coastal plain sands of Calabar area (Southern Nigeria) using surface resistivity and hydrogeological data. *Journal of African Earth Sciences*, 35(3), pp.433-443.
- Ekanem, A.M., George, N.J., Thomas, J.E. and Nathaniel, E.U., 2020. Empirical relations between aquifer geohydraulic–geoelectric properties derived from surficial resistivity measurements in parts of Akwa Ibom State, Southern Nigeria. *Natural Resources Research*, 29, pp.2635-2646.
- Esu, E.O., Okereke, C.S. and Edet, A.E., 1999. A regional hydrostratigraphic study of Akwa Ibom State, southeastern Nigeria. *Global Journal of Pure and Applied Sciences*, 5, pp.89-96.
- Fetter, C.W., 2018. *Applied hydrogeology*. Waveland Press.
- George, N., Obianwu, V. and Udofia, K., 2011. Estimation of aquifer hydraulic parameters via complementing surficial geophysical measurement by laboratory measurements on the aquifer core samples. *International Review of Physics*, 5(2), pp.88-97.
- George, N.J., Ekanem, A.M., Ibanga, J.I. and Udosen, N.I., 2017. Hydrodynamic implications of aquifer quality index (AQI) and flow zone indicator (FZI) in groundwater abstraction: a case study of coastal hydro-lithofacies in South-eastern Nigeria. *Journal of Coastal Conservation*, 21, pp.759-776.
- George, N.J., Ekanem, K.R., Ekanem, A.M., Udosen, N.I. and Thomas, J.E., 2022. Generic comparison of ISM and LSIT interpretation of geo-resistivity technology data, using constraints of ground truths: a tool for efficient explorability of groundwater and related resources. *Acta Geophysica*, 70(3), pp.1223-1239.
- Gopalan, C.V., 2011. A comparative study of the groundwater potential in hard rock areas of Rajapuram and Balal, Kasaragod, Kerala. *J. Ind. Geophys. Union*, 15(3), pp.179-186.
- Ibanga, J.I. and George, N.J., 2016. Estimating geohydraulic parameters, protective strength, and corrosivity of hydrogeological units: a case study of ALSCON, IkotAbasi, southern Nigeria. *Arabian Journal of Geosciences*, 9, pp.1-16.

- Ibuot, J.C., Okeke, F.N., George, N.J. and Obiora, D.N., 2017. Geophysical and physicochemical characterization of organic waste contamination of hydrolithofacies in the coastal dumpsite of Akwa Ibom State, Southern Nigeria. *Water Science and Technology: Water Supply*, 17(6), pp.1626-1637.
- Ibuot, J.C. and Obiora, D.N., 2021. Estimating geohydrodynamic parameters and their implications on aquifer repositories: a case study of University of Nigeria, Nsukka, Enugu State. *Water Practice & Technology*, 16(1), pp.162-181.
- Inim, I.J., Udosen, N.I., Tijani, M.N., Affiah, U.E. and George, N.J., 2020. Time-lapse electrical resistivity investigation of seawater intrusion in coastal aquifer of Ibeno, Southeastern Nigeria. *Applied Water Science*, 10(11), pp.1-12.
- Kouassi, F.W., Kouassi, K.A., Coulibaly, A., Kamagaté, B. and Savané, I., 2017. Efficiency of inverse slope method in the interpretation of electrical resistivity soundings data of schlumberger type. *International Journal of Engineering & Science Research*, 7, pp.121-130.
- Lobo-Ferreira, J.P., Chachadi, A.G., Diamantino, C. and Henriques, M.J., 2005. Assessing aquifer vulnerability to seawater intrusion using GALDIT Method. Part 1: application to the Portuguese aquifer of Monte Gordo. *Journal of Geosciences*, 7, pp.4059-4077.
- Narayan, P.S. and Ramanujachary, K.R., 1967. An inverse slope method of determining absolute resistivity. *Geophysics*, 32(6), pp.1036-1040.
- Niwas, S., Tezkan, B. and Israil, M., 2011. Aquifer hydraulic conductivity estimation from surface geoelectrical measurements for Krauthausen test site, Germany. *Hydrogeology Journal*, 19(2), p.307.
- Okereke, C.S., Esu, E.O. and Edet, A.E., 1998. Determination of potential groundwater sites using geological and geophysical techniques in the Cross River State, southeastern Nigeria. *Journal of African Earth Sciences*, 27(1), pp.149-163.
- Rao, B.S.P., Rao, V.V. and Venkateswarlu, N., 2005. Geoelectrical investigations for Flyover Bridge construction in marine environment of Visakhapatnam: A case study. *J. Ind. Geophys.*, 9(1), pp.13-20.
- Reijers, T.J.A. and Petters, S.W., 1987. Depositional environments and diagenesis of Albian carbonates on the Calabar Flank, SE Nigeria. *Journal of Petroleum Geology*, 10(3), pp.283-294.
- Sattar, G.S., Keramat, M. and Shahid, S., 2016. Deciphering transmissivity and hydraulic conductivity of the aquifer by vertical electrical sounding (VES) experiments in Northwest Bangladesh. *Applied Water Science*, 6, pp.35-45.
- Shekhawat, M.S. and Chundawat, D.S., 2011. Aquifer Characteristics in and around Keoladev Ghana National Park, Bharatpur,

- Rajasthan, India. *International Journal of Earth Sciences and Engineering*, 4(1), pp.45-56.
- Short, K.C. and Stäuble, A.J., 1967. Outline of geology of Niger Delta. AAPG bulletin, 51(5), pp.761-779.
- Stacher, P., 1995. Present understanding of the Niger Delta hydrocarbon habitat. In *Geology of deltas* (pp. 257-267).
- Soupios, P.M., Kouli, M., Vallianatos, F., Vafidis, A. and Stavroulakis, G., 2007. Estimation of aquifer hydraulic parameters from surficial geophysical methods: A case study of Keritis Basin in Chania (Crete–Greece). *Journal of Hydrology*, 338(1-2), pp.122-131.
- Udosen, N.I. and George, N.J., 2018a. A finite integration forward solver and a domain search reconstruction solver for electrical resistivity tomography (ERT). *Modeling Earth Systems and Environment*, 4, pp.1-12.
- Udosen, N.I. and George, N.J., 2018b. Characterization of electrical anisotropy in North Yorkshire, England using square arrays and electrical resistivity tomography. *Geomechanics and Geophysics for Geo-Energy and Geo-Resources*, 4, pp.215-233.
- Udosen, N. and Potthast, R., 2018c. Automated optimization of electrode locations for electrical resistivity tomography. *Modeling Earth Systems and Environment*, 4, pp.1059-1083.
- Udosen, N.I., 2022. Geo-electrical modeling of leachate contamination at a major waste disposal site in south-eastern Nigeria. *Modeling Earth Systems and Environment*, 8(1), pp.847-856.
- Uwa, U.E., Akpabio, G.T. and George, N.J., 2019. Geohydrodynamic parameters and their implications on the coastal conservation: a case study of Abak Local Government Area (LGA), Akwalbom State, Southern Nigeria. *Natural Resources Research*, 28, pp.349-367.
- Virupaksha, H.S. and Lokesh, K.N., 2021. Electrical resistivity, remote sensing and geographic information system approach for mapping groundwater potential zones in coastal aquifers of Gurpur watershed. *Geocarto International*, 36(8), pp.888-902.
- Yadav, S.P., Singh, D.N., Singh, A.K. and Prasad, R., 2009. Electrical resistivity imaging for the study of quartz reef using inverse slope method. *Current Science*, pp.1521-1527.